Deficiency of Glycine *N*-Methyltransferase Aggravates Atherosclerosis in Apolipoprotein E–Null Mice

Chien-Yu Chen,[1] Li-Chieh Ching,[1] Yi-Jen Liao,[2] Yuan-Bin Yu,[3] Chia-Yuan Tsou,[1] Song-Kun Shyue,[4] Yi-Ming Arthur Chen,[2] and Tzong-Shyuan Lee[1,5]

[1]Department of Physiology, School of Medicine, National Yang-Ming University, Taipei, Taiwan; [2]Department of Microbiology, School of Medicine, National Yang-Ming University, Taipei, Taiwan; [3]Division of Hematology and Oncology, Taipei Veterans General Hospital, Taipei, Taiwan;[4]Cardiovascular Division, Institute of Biomedical Sciences, Academia Sinica, Taipei, Taiwan; and [5]Brain Research Center, National Yang-Ming University, Taipei, Taiwan

The mechanism underlying the dysregulation of cholesterol metabolism and inflammation in atherogenesis is not understood fully. Glycine *N*-methyltransferase (GNMT) has been implicated in hepatic lipid metabolism and the pathogenesis of liver diseases. However, little is known about the significance of GNMT in atherosclerosis. We showed the predominant expression of GNMT in foamy macrophages of mouse atherosclerotic aortas. Genetic deletion of *GNMT* exacerbated the hyperlipidemia, inflammation and development of atherosclerosis in apolipoprotein E–deficient mice. In addition, ablation of *GNMT* in macrophages aggravated oxidized low-density lipoprotein-mediated cholesterol accumulation in macrophage foam cells by downregulating the expression of reverse cholesterol transporters including ATP-binding cassette transporters-A1 and G1 and scavenger receptor BI. Furthermore, tumor necrosis factor-α–induced inflammatory response was promoted in *GNMT*-null macrophages. Collectively, our data suggest that GNMT is a crucial regulator in cholesterol metabolism and in inflammation, and contributes to the pathogenesis of atherosclerosis. This finding may reveal a potential therapeutic target for atherosclerosis.

INTRODUCTION

Glycine *N*-methyltransferase (GNMT) catalyzes the synthesis of sarcosine from glycine with *S*-adenosylmethionine (SAM) used as the methyl donor and thereby is an important regulator in the metabolism of SAM and *S*-adenosylhomocysteine (SAH) in the liver (1,2). In addition to its enzyme activity, GNMT functions as a folate-binding protein and cytosolic receptor for environmental carcinogens by activating hepatic detoxification pathways (3–5). Considerable evidence supports that GNMT critically modulates the pathogenesis of liver dis-

eases (6–8). For instance, GNMT is a tumor suppressor and is downregulated in patients with liver cirrhosis or hepatocellular carcinoma (HCC) (7,8). Moreover, clinical studies demonstrated metabolic abnormalities, including increased levels of serum methionine, SAM, and triglycerides, and hepatitislike symptoms in *GNMT*-deficient patients (9,10). Likewise, a *GNMT*-knockout (*GNMT*^{−/−}) mouse model exhibited the same phenotype of liver diseases, including chronic hepatitis, steatosis, fibrosis and spontaneous HCC development (11–13). The level of serum cholesterol is elevated in

both *GNMT*-deficient patients and *GNMT*^{−/−} mice, which implies that GNMT may be involved in the regulation of cholesterol metabolism (9,11). However, little is known about the role of GNMT in hypercholesterolemia and related diseases such as atherosclerosis.

Atherosclerosis is a chronic inflammatory disease of multiple etiologies resulting from excessive lipid accumulation and a persistent chronic inflammatory process within the artery wall (14). Although the detailed mechanisms of this disease are not defined fully, dysregulation of cholesterol metabolism and inflammatory response mediated by lipid-laden macrophages has a major role in the initiation and progression of atherosclerosis (14–16). In atherosclerotic lesions, macrophages engulf oxidized low-density lipoprotein (oxLDL) via scavenger receptors (SRs) such as class A SR (SR-A) or CD36 (17–19). Conversely, the efflux of intracellular cholesterol to high-density lipoprotein (HDL) is mediated by reverse cholesterol transporters (RCTs) in-

Address correspondence to *Tzong-Shyuan Lee, Department of Physiology, National Yang-Ming University, Taipei 11221, Taiwan; Phone: +886-2-28267365, Fax: +886-2-28264049, E-mail: tslee@ym.edu.tw; or Yi-Ming Arthur Chen, Department of Microbiology, School of Medicine, National Yang-Ming University, Taipei 11211, Taiwan; Phone: +886-2-28267193, Fax: +886-2-28270576, E-mail: arthur@ym.edu.tw.*
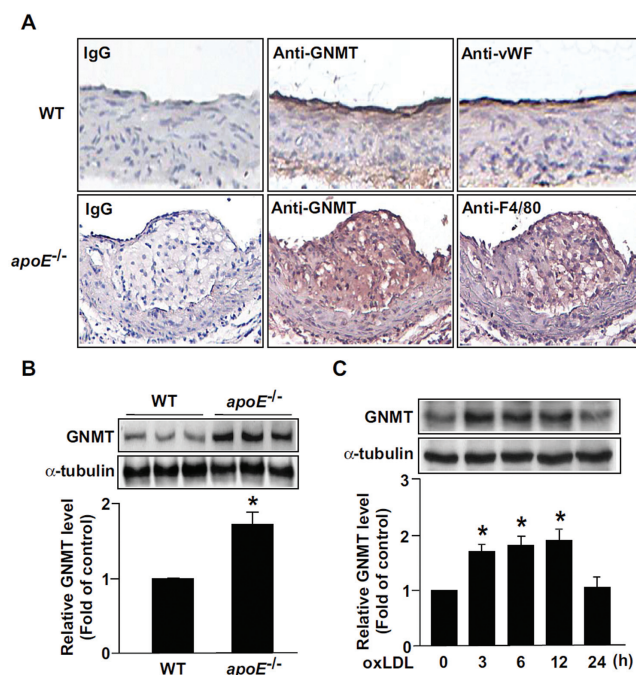
Figure 1. Expression of GNMT is elevated in the aortas of *apoE*^{−/−} mice. A) Aortic specimens from WT and 5-month-old *apoE*^{−/−} mice were immunostained with anti-GNMT, anti-vWF or anti-F4/80 antibody and then recognized by the corresponding horseradish peroxidase-conjugated secondary antibody. Antigenic sites were visualized by the addition of DAB. Hematoxylin was used for counterstaining. The vWF-positive cells and F4/80-positive cells (brown color) denoted endothelial cells and macrophages, respectively. Magnification: 100×. B) Western blot analysis of protein expression of GNMT in aortic lysates from WT and *apoE*^{−/−}. α-Tubulin was a loading control. C, Western blot analysis of GNMT protein expression in BMDMs treated with 50 µg/mL oxLDL for the indicated times. Data are mean ± SEM from five independent experiments. *$P < 0.05$ versus WT mice or vehicle-treated group.

cluding SR-BI and ATP-binding cassette transporters A1 and G1 (ABCA1 and ABCG1) (20–22). These lipid-laden macrophages also play a crucial role in the regulation of local inflammation by secreting various proinflammatory mediators (15,23,24). Therefore, therapeutic approaches to reduce foam cell formation may represent an important strategy for preventing and treating atherosclerosis (25). However, studies investigating the potential associations among GNMT, macrophages and atherosclerosis are limited.

In the present study, we investigated the role of GNMT in atherosclerosis and its underlying molecular mechanisms *in vitro* and *in vivo*. Genetic deletion of *GNMT* exacerbated the dysregulation of cholesterol efflux and inflammation in

macrophages, thus leading to accelerated progression of atherosclerosis in apolipoprotein E–deficient (*apoE*^{−/−}) mice. These findings suggest the antiatherogenic property of GNMT and its potential therapeutic relevance in cardiovascular diseases.

MATERIALS AND METHODS

Reagents and Assay Kits

Mouse anti-GNMT monoclonal antibody (Ab) was produced as described previously (26). Rabbit anti-von Willebrand factor (vWF), anti-inducible nitric oxide synthase (iNOS), anti-endothelial nitric oxide synthase (eNOS), anti-CD36, anti-ABCG1, anti-ABCG5, anti-ABCG8, anti-CD3, goat anti-vascular cell adhesion molecule-1 (VCAM-1) and anti-

SR-A Abs were from Santa Cruz Biotechnology (Santa Cruz, CA, USA). Rabbit anti-phospho-eNOS at Ser1179 Ab was from Cell Signaling Technology (Beverly, MA, USA). Rat anti-F4/80, mouse anti-ABCA1, anti-α-actin and rabbit anti-SR-BI Abs were from Abcam (Cambridge, MA, USA). Mouse anti-α-tubulin Ab, Trichrome stain kit and human LDL were from Sigma (St. Louis, MO, USA). Macrophage colony-stimulating factor (M-CSF) and enzyme-linked immunosorbent assay (ELISA) kits were from R&D (Minneapolis, MN, USA). Cholesterol and triglyceride assay kits were from Randox (Antrim, UK). Dil-labeled oxLDL was from Biomedical Technologies (Stoughton, MA, USA). NBD-cholesterol and TO901317 were from Cayman Chemical (Ann Arbor, MI, USA). Terminal deoxynucleotidyl transferase dUTP nick end labeling (TUNEL) assay kit was from Boehringer Mannheim Corp (Pleasanton, CA, USA).

Animals

All animal experiments were approved by the Animal Care and Utilization Committee of National Yang-Ming University. Wild-type (WT) mice in a C57BL/6 background were purchased from the National Laboratory Animal Center, National Science Council (Taipei, Taiwan); *apoE*^{−/−} mice were from Jackson Laboratory (Bar Harbor, MN, USA); *GNMT*^{−/−} mice in a C57BL/6 background were generated as described previously (11). *apoE*^{−/−}*GNMT*^{−/−} mice were generated by cross-breeding *apoE*^{−/−} and *GNMT*^{−/−} mice. All experimental mice were fed with a chow diet and euthanized by CO_2 at 5 months of age. Hearts, aortas and livers were isolated and subjected to further experiments.

Immunohistochemical and Histological Assessment

Heart, liver and aorta tissue blocks were cut into 8-µm sections and subjected to immunohistochemistry. Sections were reacted with 3% H_2O_2. After a blocking with 1% BSA for 30 min, samples were incubated with primary Abs at
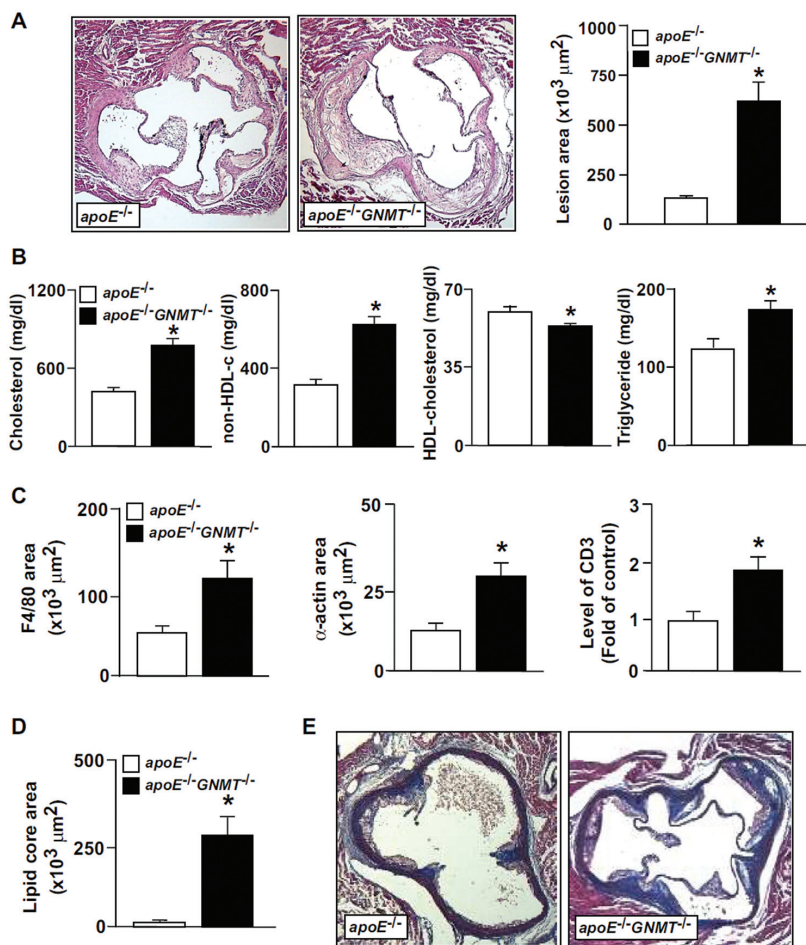
Figure 2. Knockout of *GNMT* enhances the development of atherosclerosis and abnormality of the lipid profile in *apoE$^{-/-}$* mice. *ApoE$^{-/-}$* mice (n = 14) and *apoE$^{-/-}$GNMT$^{-/-}$* mice (n = 14) were fed a chow diet for 20 wks before euthanization. A) Histology and quantification of atherosclerotic lesions in aortic roots were performed as described in Materials and Methods. Magnification: 40×. B) Analysis of serum levels of total cholesterol, non–HDL-c, HDL-c and triglycerides in *apoE$^{-/-}$* and *apoE$^{-/-}$GNMT$^{-/-}$* mice. C) The content of macrophages, smooth muscle cells (SMCs) and T cells in atherosclerotic lesions. D and E) The content of lipid core and collagen in atherosclerotic lesions. * *P* < 0.05 versus *apoE$^{-/-}$* mice.

4°C overnight and then corresponding horseradish peroxidase-conjugated secondary Ab for an additional 1 h. Antigenic sites were visualized by adding 3,3-diaminobenzidine. Hematoxylin was used for counterstaining. For histological examination, deparaffinized sections underwent hematoxylin and eosin (H&E) staining and were viewed under a Motic TYPE 102M microscope (Motic Images, China). Quantification of atherosclerotic lesions and the content of the cellular or noncellular composition were analyzed

by imaging software (Motic Images Plus 2.0, China).

TUNEL Assays

TUNEL staining was performed according to the manufacturer's instructions. Briefly, after incubation with proteinase K (10 µg/mL) for 20 min, sections were incubated with digoxigenin (DIG)-dUTP and terminal deoxynucleotidyl transferase, which catalyzes the addition of deoxyribonucleotide to 3'-OH ends of DNA fragments. The incorporation of

DIG-dUTP into DNA was visualized under a Nikon TE2000-U florescence microscope (Tokyo, Japan). Cells with clear nuclear labeling were defined as apoptotic cells.

Western Blot Analysis

Tissues or cells were lysed with lysis buffer. After centrifugation at 12,000*g*, the supernatants were collected for analysis. Aliquots of sample lysates were separated on SDS-PAGE and then transblotted on an Immobilon-P membrane. After being blocked with 5% skim milk for 1 h at room temperature, blots were incubated with primary Abs overnight and then with corresponding secondary Ab for 1 h. The protein bands were detected by use of an enhanced chemiluminescence kit (PerkinElmer, Boston, MA, USA) and quantified by use of ImageQuant 5.2 software (Healthcare BioSciences, PA, USA).

Preparation of Bone Marrow-Derived Macrophages (BMDMs)

Mononuclear cells from mice femurs and tibias were harvested by Percol (1.073 g/cm^3) density gradient centrifugation and then cultured in Minimum Essential Medium α (MEMα) supplemented with M-CSF (50 ng/mL), penicillin (100 U/mL)/streptomycin (100 µg/mL) and 10% fetal bovine serum (FBS) for 5 d.

Oxidation of LDL

Oxidation of LDL was performed as described (27). LDL was exposed to 5 µM CuSO$_4$ for 24 h at 37°C, and Cu^{2+} was removed by extensive dialysis. The extent of modification was determined by measuring thiobarbituric acid-reactive substances (TBARs).

Serum Lipid Profile Analysis

Blood was collected by cardiac puncture. After clotting and centrifugation, serum was isolated and the levels of cholesterol, HDL cholesterol (HDL-c) and triglycerides were measured by use of Spotchem EZ SP 4430 (ARKRAY Inc., Kyoto, Japan).
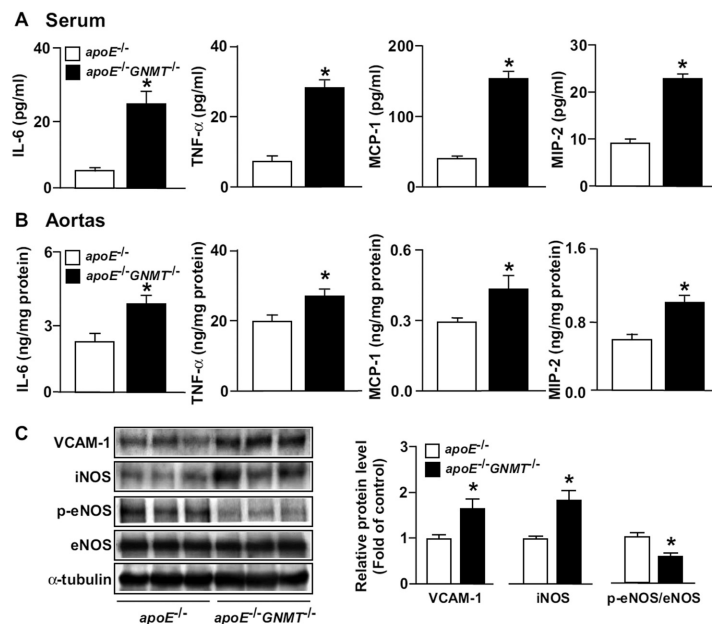
Figure 3. ApoE$^{-/-}$GNMT$^{-/-}$ mice show exacerbated inflammatory response. A and B) ELISA analysis of serum levels of IL-6, TNF-α, MCP-1 and MIP-2 in serum and aortas of apoE$^{-/-}$ mice and apoE$^{-/-}$GNMT$^{-/-}$ mice. C, Western blot analysis and quantitation of VCAM-1, inducible iNOS, phosphorylated eNOS (p-eNOS) and eNOS in aortic lysates from apoE$^{-/-}$ and apoE$^{-/-}$GNMT$^{-/-}$ mice. α-Tubulin was a loading control. Data are mean ± SEM from 14 animals. *P < 0.05 versus apoE$^{-/-}$ mice.

Cholesterol and Triglyceride Measurement in Hepatic Tissue and Macrophages

Hepatic tissues or cellular cholesterol and triglycerides were extracted by use of hexane/isopropanol (3:2, v/v). After drying, the levels of cholesterol and triglycerides were measured by colorimetric assay kits.

Oil Red O Staining

Cells were fixed with 4% paraformaldehyde and then stained with 0.5% oil red O. Hematoxylin was used for counterstaining.

Dil-oxLDL Binding Assay

Dil-oxLDL, copper-oxidized LDL, labeled with green fluorescence, has been used for experiments of oxLDL binding to SRs of macrophages (28). BMDMs from WT or GNMT$^{-/-}$ mice were incubated with Dil-oxLDL (10 µg/mL) at 4°C for 4 h. Cells were washed and lysates were analyzed by fluorometry (Molecu-

lar Devices) with 514-nm excitation and 550-nm emission.

Cholesterol Efflux Assay

Cholesterol efflux assay involved use of fluorescent NBD-cholesterol as described (27). BMDMs were incubated with oxLDL for 12 h, then NBD-cholesterol (1µ/mL) was added for an additional 6 h. NBD-cholesterol–labeled cells were washed with PBS and incubated in MEMα for another 6 h. The fluorescence-labeled cholesterol released from BMDMs into the medium was measured by use of a multilabel counter (PerkinElmer, Waltham, MA, USA). *In vivo* cholesterol efflux was performed as described previously with modifications (29). Briefly, after removing the apoB-containing lipoproteins from plasma, the apoB-derived supernatant was as the high-density lipoprotein fraction and diluted to 2.8% (equivalent to 2% serum) in cultured medium. Cholesterol efflux was measured as the difference in release of

fluorescence-labeled cholesterol released from vehicle-treated BMDMs or TO901317-treated BMDMs

Measurement of Inflammatory Cytokines

The concentrations of proinflammatory cytokines including interleukin-6 (IL-6), tumor necrosis factor-α (TNF-α), monocyte chemoattractant protein-1 (MCP-1) and macrophage inflammatory protein-2 (MIP-2) in culture medium, serum or aortas were measured by use of ELISA kits according to the manufacturer's instructions.

Statistical Analysis

The Mann-Whitney test was used to compare two independent groups. The Kruskal-Wallis test followed by the Bonferroni *post hoc* analyses were used to account for multiple testing. Analysis involved use of SPSS v8.0 (SPSS Inc, Chicago, IL, USA). *P* < 0.05 was considered statistically significant.

All supplementary materials are available online at www.molmed.org.

RESULTS

GNMT Is Expressed in Atherosclerotic Lesions of *ApoE*$^{-/-}$ Mice

To elucidate the possible involvement of GNMT in atherogenesis, we first investigated the expression of GNMT in normal and atherosclerotic aortas. Immunohistochemistry revealed GNMT in WT mice primarily expressed in aortic endothelial cells (ECs). However, in addition to the expression of GNMT in aortic ECs of apoE$^{-/-}$ mice, GNMT expressed in atherosclerotic lesions was remarkably restricted to macrophages (Figure 1A). As shown in Figure 1B, the protein expression of GNMT was increased in the aortas of apoE$^{-/-}$ mice as compared with WT mice. Because oxLDL is a proatherogenic molecule in the development of atherosclerosis (14,15), we examined the effect of oxLDL on the expression of GNMT in macrophages. BMDMs treatment with 50 µg/mL oxLDL for up to 24 h showed
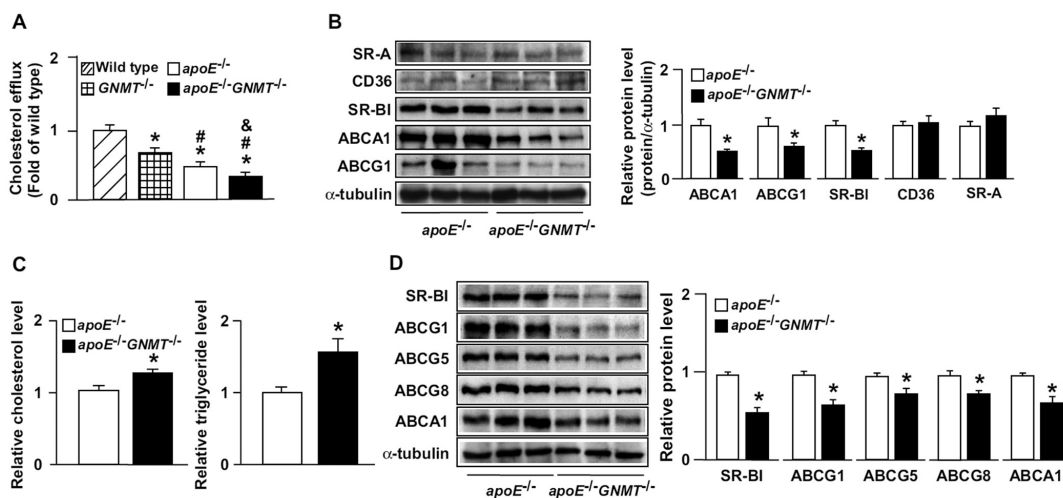
Figure 4. Deletion of *GNMT* in *apoE*^{−/−} mice impairs cholesterol metabolism in aortas and liver. A, The capacity of reverse cholesterol efflux of WT, *GNMT*^{−/−}, *apoE*^{−/−} or *apoE*^{−/−}*GNMT*^{−/−} mice. B) Western blot analysis and quantitation of protein levels of SR-A, CD36, SR-BI, ABCA1 and ABCG1 in aortas of *apoE*^{−/−} and *apoE*^{−/−}*GNMT*^{−/−} mice. C) The hepatic concentrations of cholesterol and triglyceride were assessed by colorimetric assay kits. D) Western blot analysis and quantitation of protein expression of SR-BI, ABCG1, ABCG5, ABCG8, ABCA1 in mouse liver. α-Tubulin was a loading control. Data are mean ± SEM from 14 mice. *P < 0.05 versus WT mice or *apoE*^{−/−} mice, #P < 0.05 versus *GNMT*^{−/−} mice, &P < 0.05 versus *apoE*^{−/−} mice.

time-dependently increased expression of GNMT (Figure 1C). The expression occurred as early as 3 h after treatment, peaked at 12 h and then declined to the basal level. Thus, GNMT may play an important role in the development of atherosclerosis.

Deficiency of *GNMT* Exacerbates the Development of Atherosclerosis, Hyperlipidemia and Inflammation in *ApoE*^{−/−} Mice

To delineate the potential role of GNMT in the pathogenesis of atherosclerosis, *apoE*^{−/−} mice and *apoE*^{−/−}*GNMT*^{−/−} mice were used as *in vivo* models. Genetic deletion of *GNMT* in *apoE*^{−/−} mice greatly enhanced the development of atherosclerotic lesions as compared with *apoE*^{−/−}-alone mice (Figure 2A). Furthermore, serum levels of total cholesterol, non–HDL cholesterol (non–HDL-c) and triglycerides were increased significantly and level of HDL-c was decreased in male *apoE*^{−/−}*GNMT*^{−/−} mice (Figure 2B). The cellular and noncellular composition of atherosclerotic plaque such as the content of macrophages, smooth muscle cells (SMCs), T cells, lipid core and collagen also was increased in *apoE*^{−/−}*GNMT*^{−/−}

mice (Figures 2C, D and Supplementary Figure S1). Moreover, the macrophage apoptosis was enhanced in atherosclerotic lesions of *apoE*^{−/−}*GNMT*^{−/−} mice as revealed by TUNEL assays (Supplementary Figure S2). Previous studies have demonstrated that inflammation within atherosclerotic lesions is a central event in the progression of atherosclerosis (15,23,24). We next examined whether GNMT was involved in the regulation of the inflammatory response during atherogenesis. As compared with *apoE*^{−/−} mice, *apoE*^{−/−}*GNMT*^{−/−} mice showed elevated levels of IL-6, TNF-α, MCP-1 and MIP-2 in serum and aortas (Figures 3A, B), all important proatherogenic molecules. Endothelial cell (EC) dysfunction, the earliest event in the development of atherosclerosis, is characterized by impaired eNOS activation and increased expression of adhesion molecules such as VCAM-1 (14,16), and iNOS plays a key role in vascular inflammation in atherosclerotic lesions (19). We further showed the expression of VCAM-1 and iNOS in aortas were higher and eNOS phosphorylation was lower in *apoE*^{−/−}*GNMT*^{−/−} than *apoE*^{−/−} mice (Figure 3C). Thus, GNMT may have a vital role in the regulation of

lipid metabolism and inflammatory response during atherogenesis.

Knockout of *GNMT* Impairs Reverse Cholesterol Transport and Cholesterol Elimination in *ApoE*^{−/−} Mice

Reverse cholesterol transport from peripheral tissues to the liver is a critical pathway for cholesterol clearance (20–22). Once the free cholesterol or phospholipid is transferred to apolipoprotein A-I (apoA-I) or HDL, these lipids can be further delivered to the liver for excretion (30). Liver SR-BI mediates the selective uptake of cholesterol ester from HDL and thus promotes the excretion of cholesterol into bile, which leads to the elimination of excessive cholesterol (30). Two ABC transporters, ABCG5 and ABCG8, are responsible for the elimination of cholesterol by the liver (31). Our data demonstrated that deletion of *GNMT* in WT mice or *apoE*^{−/−} mice impaired the reverse cholesterol efflux (Figure 4A). Additionally, deletion of *GNMT* in *apoE*^{−/−} mice decreased the expression of the SR-BI, ABCA1 and ABCG1 without changing the expression of SR-A and CD36 in mouse aortas (Figure 4B). Epidemiological investigations suggest that dysregulation of lipid metabolism in
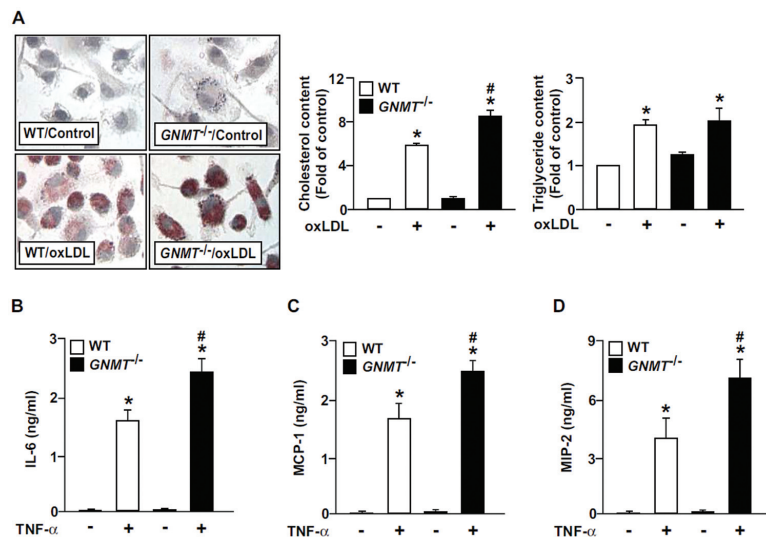
Figure 5. Deficiency of *GNMT* accelerates lipid accumulation in macrophage foam cells. A) Oil red O and hematoxylin staining of BMDMs from WT and *GNMT*$^{-/-}$ mice incubated with or without oxLDL (50 μg/mL) for 24 h. Magnification: 40×. Levels of cholesterol and triglycerides analyzed by colorimetric assay kits. B) BMDMs from WT and *GNMT*$^{-/-}$ mice were treated with vehicle or TNF-α (10 ng/mL) for 24 h. After incubation, cell culture media was collected and the production of IL-6, MCP-1 and MIP-2 was evaluated by ELISA. Data are mean ± SEM from 5 independent experiments. *$P < 0.05$ versus WT vehicle-treated group, #$P < 0.05$ versus WT oxLDL-treated or TNF-α-treated group.

liver is an important risk factor for atherosclerosis (14,15). More recently, several lines of evidence show *GNMT*$^{-/-}$ mice with fatty liver, liver fibrosis and inflammation and ultimately HCC (11–13). We further demonstrated that the hepatic accumulation of lipids including cholesterol and triglycerides was higher in *apoE*$^{-/-}$*GNMT*$^{-/-}$ than *apoE*$^{-/-}$ mice (Figure 4C). Moreover, the hepatic protein levels of SR-BI, ABCA1 and ABCG1 were decreased markedly in *apoE*$^{-/-}$*GNMT*$^{-/-}$ mice (Figure 4D). As well, the protein levels of ABCG5 and ABCG8 were significantly reduced in the liver of *apoE*$^{-/-}$*GNMT*$^{-/-}$ mice (see Figure 4D). These results show that GNMT is a crucial regulator of cholesterol transport in peripheral tissues and cholesterol elimination in liver.

Deletion of *GNMT* Exaggerates OxLDL-Induced Lipid Accumulation and TNF-α-Induced Inflammation in Macrophages

Because GNMT was upregulated by oxLDL in macrophages, we speculated that GNMT is involved in oxLDL-induced foam cell formation. As shown in Figure 5A, oxLDL-induced lipid accumulation was significantly higher in *GNMT*$^{-/-}$ than WT macrophages. This increase in intracellular lipid accumulation in *GNMT*$^{-/-}$ macrophages also was shown by an increase in cellular level of cholesterol but not triglycerides (Figure 5A). In addition, the TNF-α induction of proinflammatory mediators such as IL-6, MCP-1 and MIP-2 were augmented significantly in *GNMT*$^{-/-}$ macrophages (Figures 5B–D). However, deletion of *GNMT* did not affect the migratory capacity of macrophages in response to the treatment with M-CSF or oxLDL (data not shown). Because cellular cholesterol content in macrophage foam cells is dynamically regulated by oxLDL uptake and cholesterol efflux via SRs and RCTs, respectively (17–22), we examined the role of GNMT in regulating cholesterol homeostasis and the expression of SRs and RCTs. Deletion of *GNMT* impaired cholesterol efflux with-

out affecting oxLDL binding (Figure 6A). Moreover, the protein levels of RCTs such as SR-BI, ABCA1, and ABCG1 were significantly lower in oxLDL-treated *GNMT*$^{-/-}$ than oxLDL-treated WT macrophages. In contrast, ablation of *GNMT* did not affect the protein levels of SR-A or CD36 after oxLDL treatment (Figure 6B). Thus, GNMT participates in the regulation of cholesterol metabolism and the inflammatory response in response to proatherogenic stimuli in macrophages.

DISCUSSION

GNMT was first identified in the liver to function as a key regulator in SAM/SAH metabolism, activation of liver detoxification and the development of HCC (2,5,12,13). However, the pathophysiological role of GNMT in cardiovascular diseases such as atherosclerosis has never been defined. Here we showed that genetic deletion of *GNMT* exacerbated the dysregulation of cholesterol metabolism and the inflammatory response in the aorta of the hyperlipidemic mouse model, which led to the progression of atherosclerosis. In addition, deficiency of *GNMT* impaired the RCT-dependent cholesterol efflux and hence promoted the cholesterol accumulation on oxLDL challenge in macrophages. Consistently, TNF-α-induced production of proinflammatory cytokines was upregulated in *GNMT*$^{-/-}$ macrophages. The observations support the novel role of GNMT in atherosclerosis. Therefore, GNMT-dependent regulation is crucial for the modulation of lipid metabolism and inflammation during atherogenesis.

During the past decade, most researches into GNMT have investigated its role in tumorigenesis of hepatoma with the use of *GNMT*$^{-/-}$ mice. Interestingly, *GNMT*$^{-/-}$ mice unexpectedly exhibit elevated serum cholesterol level (11), the most important risk factor for the initiation and development of early-stage atherosclerosis. Indeed, we showed the time-dependent development of early-stage atheroma in male *GNMT*$^{-/-}$ mice (Supplementary Figure S3) and an
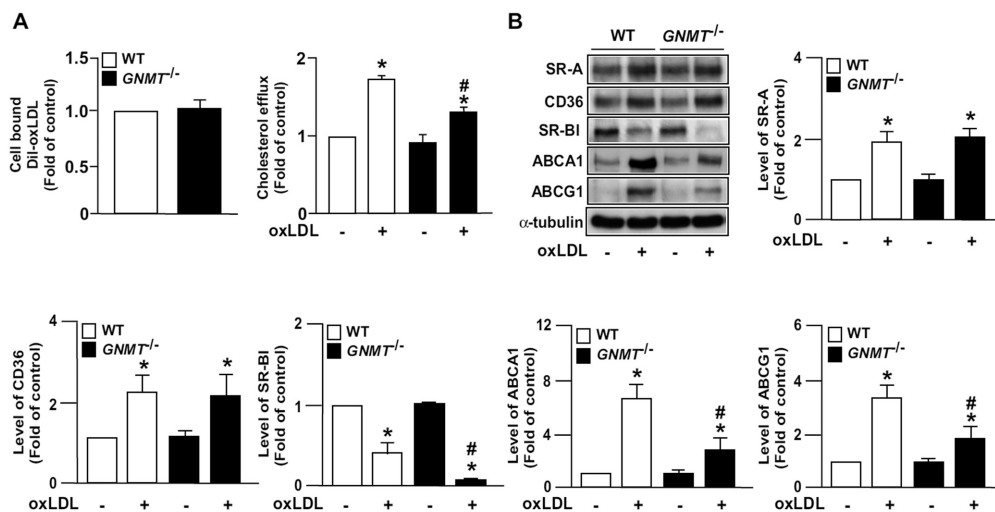
Figure 6. Loss of *GNMT* impairs RCT-dependent cholesterol efflux in macrophages. A) For Dil-oxLDL binding assay, BMDMs from WT and *GNMT$^{-/-}$* mice were incubated with Dil-labeled oxLDL at 4°C for 4 h, then fluorescence was determined. For cholesterol efflux assay, BMDMs from WT and *GNMT$^{-/-}$* mice were treated with or without oxLDL (50 μg/mL) for 12 h and then with NBD-cholesterol for another 6 h. Cholesterol efflux was defined as the fluorescence in medium from each group. B) BMDMs were treated with or without oxLDL (50 μg/mL) for 24 h. Western blot analysis and quantitation of the protein expression of SR-A, CD36, SR-BI, ABCA1, and ABCG1. α-Tubulin was a loading control. Data are mean ± SEM from five independent experiments. *$P < 0.05$ versus WT nontreated group, #$P < 0.05$ versus WT oxLDL-treated group.

exacerbation of atherosclerosis in male *apoE$^{-/-}$GNMT$^{-/-}$* mice compared with *apoE$^{-/-}$* mice. Similar to the observations in male *apoE$^{-/-}$GNMT$^{-/-}$* mice, genetic deletion of GNMT in female *apoE$^{-/-}$* mice increased the lesion size of atherosclerosis by ~5-fold (Supplementary Figure S4), suggesting the effect of *GNMT* deficiency in the development of atherosclerosis may be gender independent. This finding is in contrast to our previous report that *GNMT* deficiency displays a gender-dependent effect on the pathogenesis of hepatocellular carcinoma (11). Although the detail mechanism was unclear, we thought that the possible explanation for the discrepancy between these two studies may be due to the different disease models. Additionally, GNMT activation has important consequences for the metabolism of homocysteine, also a risk factor for atherosclerosis (32). More recently, Varela-Rey *et al*. demonstrated that deletion of *GNMT* in mice impaired liver regeneration because of dysregulation of multiple signaling pathways including nuclear factor-κB, signal transducer and activator of transcription-3, eNOS, and iNOS (33), all important regu-

lators of inflammation during the development of atherosclerosis. These observations strongly suggest that GNMT might have a role in the development of atherosclerosis other than in SAM/SAH metabolism and liver diseases.

We created *apoE$^{-/-}$GNMT$^{-/-}$* mice and isolated BMDMs from WT and *GNMT$^{-/-}$* mice as our *in vivo* and *in vitro* models to explore the possible involvement of GNMT and its molecular mechanisms in atherosclerosis. Our *in vivo* data showed exacerbated atherosclerotic lesions in *apoE$^{-/-}$GNMT$^{-/-}$* mice as compared with *apoE$^{-/-}$* mice, which suggests the critical role of GNMT in atherogenesis. This notion was further supported by loss of *GNMT*, further augmenting the abnormalities of lipid metabolism and inflammatory response, two key events in the progression of atherosclerosis, under the hyperlipidemic condition. Additionally, *apoE$^{-/-}$GNMT$^{-/-}$* mice exhibited a decrease in body weight (BW) and ratio of white adipose tissue weight to BW as compared with *apoE$^{-/-}$* mice (Supplementary Figure S5). These *in vivo* findings suggest that GNMT negatively modulates the dysregulation of lipid

metabolism and inflammation in *apoE$^{-/-}$* mice.

Similarly, *in vitro* results suggested that the increase in lipid accumulation induced by oxLDL was further augmented in *GNMT$^{-/-}$* macrophages because of the reduced cholesterol efflux. The intracellular cholesterol homeostasis of foam cells is tightly regulated by cholesterol uptake and efflux, and these processes are controlled by SRs and RCTs, respectively (34). Deficiency of *GNMT* did not affect cholesterol uptake on Dil-oxLDL binding assay or expression of SR-A and CD36, two key SRs involved in the internalization of modified LDL (17–19). In contrast, *GNMT$^{-/-}$* macrophages were defective in oxLDL-elicited RCT-cholesterol efflux. Although the precise mechanism underlying the dysfunction in cholesterol efflux caused by *GNMT* deletion is poorly understood, our data showed that increased foam cell formation by *GNMT* deletion is likely mediated by reduced RCT-mediated cholesterol efflux but not cholesterol uptake in macrophages.

Once free cholesterol or phospholipids are transferred to HDL or apoA-I, these lipids can be further delivered to the

liver for excretion by binding to the HDL receptor SR-BI of hepatocytes (30). Liver SR-BI mediates the selective uptake of cholesterol ester from HDL, thus promoting the excretion of cholesterol into bile via ABCG5 and ABCG8, which leads to elimination of excessive cholesterol (30,31). Therefore, we next asked whether GMNT also affected the cholesterol elimination and expression of cholesterol transporters such as SR-BI, ABCG1, ABCG5, ABCG8 and ABCA1 in liver. Intriguingly, all these transporters were downregulated in liver tissues of $apoE^{-/-}GNMT^{-/-}$ mice as compared with $apoE^{-/-}$ mice, so GNMT may be a crucial link in reverse cholesterol transport between the aorta and liver.

Ample evidence indicates that the loss or impairment of RCT function in human or experimental animals indeed causes hyperlipidemia, abnormal inflammatory response and excessive cholesterol deposition in peripheral tissues, including aortas (35–37). For example, several epidemiological studies demonstrated increased morbidity and mortality from cardiovascular complications in patients with Tangier disease, with low levels of ABCA1 transporter (35,38). Growing evidence also suggests that inflammation downregulates ABCA1 expression by an unclear mechanism *in vitro* and *in vivo* (39,40). In addition, the mRNA expression of GNMT is upregulated in response to lipopolysaccharide (LPS) in sea cucumbers but decreased in mice liver (41,42). Moreover, treatment with SAM was found to inhibit LPS-induced TNF-α induction in macrophages (43). Recently, Liao *et al*. reported that *GNMT* deficiency causes decreased defense to reactive oxygen species (ROS)-induced oxidative stress by downregulating antioxidant liver genes, including superoxide dismutase (SOD) 1, 2 and 3; catalase; peroxiredoxin-2, 5 and 6; arginase-1; regucalcin; glutathione peroxidase 1; and Cu-Zn SOD. All of these genes have been implicated in ROS production in inflammatory diseases (44). Nevertheless, whether GNMT is involved in the regulation of cholesterol metabolism and inflammation

and its mechanism in the pathogenesis of Tangier disease or inflammatory diseases remains for further investigation.

CONCLUSION

Over the past decade, increasing studies indicated that GNMT expression extended to organs other than the liver (45). Notably, we found the expression of GNMT especially localized in ECs under the normal condition and its expression in ECs was decreased under the hyperlipidemic condition in mice. Nitric oxide derived from eNOS activation participates in various vascular functions, including vessel relaxation, antiaggregation of platelets, and antiinflammation (15). However, the role of GNMT in the regulation of EC function is poorly understood. Our data showed that phosphorylated but not total eNOS was decreased in level in the aortas of $apoE^{-/-}GNMT^{-/-}$ mice, which supports the involvement of *GNMT* in modulation of eNOS activity. This result is in agreement with the finding of Varela-Rey *et al*. that GNMT knockout in mice hinders the activation of the eNOS signaling pathway, thus leading to impaired liver regeneration (33). Therefore, GNMT may be involved in regulating EC dysfunction, thought to be the earliest event in the development of atherosclerosis (14). Additionally, SR-BI is required for HDL- or estradiol-mediated eNOS activation in ECs (46). Our data further demonstrated that *GNMT* deficiency resulted in the downregulation of SR-BI in the mouse aorta and liver. Whether this decrease in SR-BI expression is attributed to eNOS inactivation in $GNMT^{-/-}$ mice needs further investigation. In summary, this study demonstrates the novel role of GNMT in regulating lipid metabolism and inflammation *in vitro* and *in vivo*. Our findings suggest that GNMT may be a valuable therapeutic target for treating or preventing atherosclerosis or other inflammatory diseases.

ACKNOWLEDGMENTS

DISCLOSURE

The authors declare that they have no competing interests as defined by Molecular Medicine, or other interests that might be perceived to influence the results and discussion reported in this paper.

REFERENCES

1. Heady JE, Kerr SJ. (1973) Purification and characterization of glycine *N*-methyltransferase. *J. Biol. Chem.* 248:69–72.
2. Kerr SJ. (1972) Competing methyltransferase systems. *J. Biol. Chem.* 247:4248–52.
3. Cook RJ, Wagner C. (1984) Glycine *N*-methyltransferase is a folate binding protein of rat liver cytosol. *Proc. Natl. Acad. Sci. U. S. A.* 81:3631–4.
4. Bhat R, Bresnick E. (1997) Glycine *N*-methyltransferase is an example of functional diversity. Role as a polycyclic aromatic hydrocarbon-binding receptor. *J. Biol. Chem.* 272:21221–6.
5. Chen SY, *et al*. (2004) Glycine *N*-methyltransferase tumor susceptibility gene in the benzo(a)pyrene-detoxification pathway. *Cancer Res.* 64:3617–23.
6. Yen CH, *et al*. (2009) Glycine *N*-methyltransferase affects the metabolism of aflatoxin B1 and blocks its carcinogenic effect. *Toxicol. Appl. Pharmacol.* 235:296–304.
7. Chen YM, *et al*. (1998) Characterization of glycine-*N*-methyltransferase-gene expression in human hepatocellular carcinoma. *Int. J. Cancer.* 75:787–93.
8. Avila MA, *et al*. (2000) Reduced mRNA abundance of the main enzymes involved in methionine metabolism in human liver cirrhosis and hepatocellular carcinoma. *J. Hepatol.* 33:907–14.
9. Mudd SH, *et al*. (2001) Glycine *N*-methyltransferase deficiency: a novel inborn error causing persistent isolated hypermethioninaemia. *J. Inherit. Metab. Dis.* 24:448–64.
10. Augoustides-Savvopoulou P, *et al*. (2003) Glycine *N*-methyltransferase deficiency: a new patient with a novel mutation. *J. Inherit. Metab. Dis.* 26:745–59.
11. Liu SP, *et al*. (2007) Glycine *N*-methyltransferase–/– mice develop chronic hepatitis and glycogen storage disease in the liver. *Hepatology.* 46:1413–25.
12. Martínez-Chantar ML, *et al*. (2008) Loss of the glycine *N*-methyltransferase gene leads to steato-

sis and hepatocellular carcinoma in mice. *Hepatology*. 47:1191–9.

13. Liao YJ, *et al*. (2009) Characterization of a glycine *N*-methyltransferase gene knockout mouse model for hepatocellular carcinoma: Implications of the gender disparity in liver cancer susceptibility. *Int. J. Cancer*. 124:816–26.

14. Glass CK, Witztum JL. (2001) Atherosclerosis: The road ahead. *Cell*. 104:503–16.

15. Lusis AJ. (2000) Atherosclerosis. *Nature*. 407:233–41.

16. Hansson GK, Libby P, Schönbeck U, Yan ZQ. (2002) Innate and adaptive immunity in the pathogenesis of atherosclerosis. *Circ. Res*. 91:281–91.

17. Kunjathoor VV, *et al*. (2002) Scavenger receptors class A-I/II and CD36 are the principal receptors responsible for the uptake of modified low density lipoprotein leading to lipid loading in macrophages. *J. Biol. Chem*. 277:49982–8.

18. Rahaman SO, *et al*. (2006) A CD36-dependent signaling cascade is necessary for macrophage foam cell formation. *Cell Metab*. 4:211–21.

19. Witztum JL. (2005) You are right too! *J. Clin. Invest*. 115:2072–5.

20. Van Eck M, Bos IS, Hildebrand RB, Van Rij BT, Van Berkel TJ. (2004) Dual role for scavenger receptor class B, type I on bone marrow-derived cells in atherosclerotic lesion development. *Am. J. Pathol*. 165:785–94.

21. Joyce CW, *et al*. (2002) The ATP binding cassette transporter A1 (ABCA1) modulates the development of aortic atherosclerosis in C57BL/6 and apoE-knockout mice. *Proc. Natl. Acad. Sci. U. S. A*. 99:407–12.

22. Out R, *et al*. (2006) Macrophage ABCG1 deletion disrupts lipid homeostasis in alveolar macrophages and moderately influences atherosclerotic lesion development in LDL receptor-deficient mice. *Arterioscler. Thromb. Vasc. Biol*. 26:2295–300.

23. Kleemann R, Zadelaar S, Kooistra T. (2008). Cytokines and atherosclerosis: a comprehensive review of studies in mice. *Cardiovasc. Res*. 79:360–76.

24. Fazio S, Linton MF. (2001) The inflamed plaque: cytokine production and cellular cholesterol balance in the vessel wall. *Am. J. Cardiol*. 88:12–5E.

25. Li AC, Glass CK. (2002) The macrophage foam cell as a target for therapeutic intervention. *Nat. Med*. 8:1235–42.

26. Liu HH, *et al*. (2003) Characterization of reduced expression of glycine *N*-methyltransferase in cancerous hepatic tissues using two newly developed monoclonal antibodies. *J. Biomed. Sci*. 10:87–97.

27. Cheng LC, *et al*. (2011) α-Lipoic acid ameliorates foam cell formation via liver X receptor α-dependent upregulation of ATP-binding cassette transporters A1 and G1. *Free Radic. Biol. Med*. 50:47–54.

28. Han KH, *et al*. (2000) Oxidized LDL reduces monocyte CCR2 expression through pathways involving peroxisome proliferator-activated receptor gamma. *J. Clin. Invest*. 106:793–802.

29. Asztalos BF, *et al*. (2005) Differential effects of HDL subpopulations on cellular ABCA1- and SR-BI-mediated cholesterol efflux. *J. Lipid Res*. 46:2246–53.

30. Oram JF, Vaughan AM. (2006) ATP-Binding cassette cholesterol transporters and cardiovascular disease. *Circ. Res*. 99:1031–43.

31. Wittenburg H, Carey MC. (2002) Biliary cholesterol secretion by the twinned sterol half-transporters ABCG5 and ABCG8. *J. Clin. Invest*. 110:605–9.

32. Ciaccio M, Bellia C. (2010) Hyperhomocysteinemia and cardiovascular risk: effect of vitamin supplementation in risk reduction. *Curr. Clin. Pharmacol*. 5:30–6.

33. Varela-Rey M, *et al*. (2009) Impaired liver regeneration in mice lacking glycine *N*-methyltransferase. *Hepatology*. 50:443–52.

34. Rader DJ, Puré E. (2005) Lipoproteins, macrophage function, and atherosclerosis: beyond the foam cell? *Cell Metab*. 1:223–30.

35. Brooks-Wilson A, *et al*. (1999) Mutations in ABC1 in Tangier disease and familial high-density lipoprotein deficiency. *Nat. Genet*. 22:336–45.

36. Aiello RJ, *et al*. (2002) Increased atherosclerosis in hyperlipidemic mice with inactivation of ABCA1 in macrophages. *Arterioscler. Thromb. Vasc. Biol*. 22:630–7.

37. van Eck M, *et al*. (2002) Leukocyte ABCA1 controls susceptibility to atherosclerosis and macrophage recruitment into tissues. *Proc. Natl. Acad. Sci. U. S. A*. 99:6298–303.

38. Serfaty-Lacrosniere C, *et al*. (1994) Homozygous Tangier disease and cardiovascular disease. *Atherosclerosis*. 107:85–98.

39. Baranova I, *et al*. (2002) Lipopolysaccharide down regulates both scavenger receptor B1 and ATP binding cassette transporter A1 in RAW cells. *Infect. Immun*. 70:2995–3003.

40. McGillicuddy FC, *et al*. (2009) Inflammation impairs reverse cholesterol transport in vivo. *Circulation*. 119:1135–45.

41. Ramírez-Gómez F, Ortiz-Pineda PA, Rivera-Cardona G, García-Arrarás JE. (2009) LPS-induced genes in intestinal tissue of the sea cucumber *Holothuria glaberrima*. *PLoS One*. 4:e6178.

42. Ko K, *et al*. (2008) Changes in *S*-adenosylmethionine and GSH homeostasis during endotoxemia in mice. *Lab. Invest*. 88:1121–9.

43. Watson WH, Zhao Y, Chawla RK. (1999) *S*-adenosylmethionine attenuates the lipopolysaccharide-induced expression of the gene for tumour necrosis factor alpha. *Biochem. J*. 342:21–5.

44. Liao YJ, *et al*. (2010) Deficiency of glycine *N*-methyltransferase results in deterioration of cellular defense to stress in mouse liver. *Proteomics Clin. Appl*. 4:394–406.

45. Yeo EJ, Wagner C. (1994) Tissue distribution of glycine *N*-methyltransferase, a major folate-binding protein of liver. *Proc. Natl. Acad. Sci. U. S. A*. 91:210–4.

46. Yuhanna IS, *et al*. (2001) High-density lipoprotein binding to scavenger receptor-BI activates endothelial nitric oxide synthase. *Nat. Med*. 7:853–7.